

Dilatancy of frictional granular materials under oscillatory shear with constant pressure

Daisuke Ishima* and Hisao Hayakawa

Yukawa Institute for Theoretical Physics, Kyoto University, Kyoto 606-8502, Japan

(Dated: December 22, 2024)

We performed numerical simulations of a two-dimensional frictional granular system under oscillatory shear confined by constant pressure. We found that the system undergoes dilatancy as the strain is increased. We confirmed that compaction also takes place at an intermediate strain amplitude for a small mutual friction coefficient between particles. We found that compaction depends on the pressure while dilatancy little depends on the pressure.

I. INTRODUCTION

Granular materials consist of a collection of distinct macroscopic particles such as sands and glass beads. The evolution of the particles obeys Newton's equation with repulsive force between particles. In reality, due to the roughness of the particles, mutual friction between particles is unavoidable in granular systems. We call such particles frictional particles. However, we sometimes ignore the mutual friction as an idealistic model. We call such particles frictionless particles. So far many theoretical studies have only conducted for frictionless particles. Previous studies, however, pointed out that the mutual friction causes drastic changes in rheology such as the emergence of discontinuous shear thickening (DST) [1–4]. Bi et al. found that the shear jammed state is only observable in frictional particles [5]. Various researchers studied shear jammed state and DST in systems taking into account the mutual friction [6–13].

It is well known that dilatancy which is the volume expansion of a collection of particles takes place in granular systems [14–17], when shear is applied to them. More dilatant structure is realized for the high shear rate [18–21]. Previous studies also reported the existence of compaction in which repeated oscillations to the system make particles denser and more ordered configurations [22–27]. However, the influence of the mutual friction to dilatancy and compaction has not been systematically studied yet. Thus, this paper, which is complementary to the previous paper [28], focuses on appearances of dilatancy and compaction of frictional particles under oscillatory shear.

The contents of this paper are as follows. In the next section, we explain the setup of our numerical simulation. In Section III, we present our numerical results to clarify the conditions of occurrence of dilatancy and compaction. In the last section, we summarize our results.

II. SET UP OF OUR SIMULATION

We consider a two-dimensional system containing N granular particles with the mutual friction characterized

by Coulomb's friction coefficient μ . To prevent crystallization, the system contains a four-dispersion particles whose diameters are d_0 , $0.9d_0$, $0.8d_0$, and $0.7d_0$, respectively. There are $N/4$ particles for each particle size [2, 29, 30]. Since we assume that the density of each particle is identical, the mass of each particle is proportional to the square of its diameter. In our study, m_0 stands for the mass of a particle with its diameter d_0 [28].

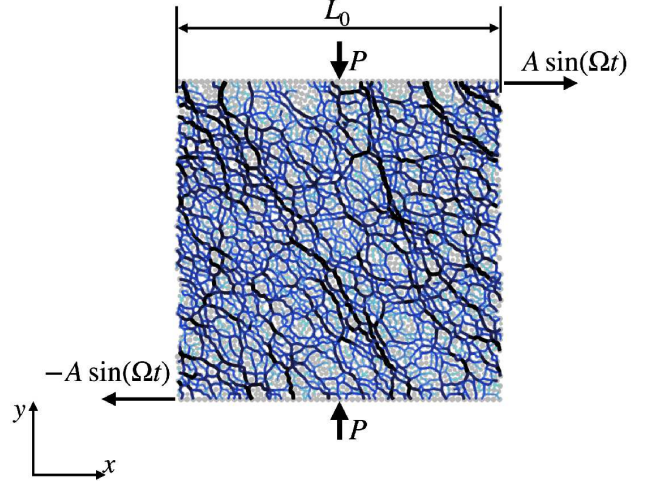


FIG. 1. A snapshot of our simulated system, where P , A and Ω are the pressure, strain amplitude, and angular frequency of oscillation, respectively. The circles and lines represent the particles and contact network of particles, respectively. The thickness of each line is proportional to the magnitude of the contact force.

We ignore the effect of gravity throughout this paper. We adopt the periodic boundary condition in the shear (x) direction and introduce mobile walls in the vertical (y) direction. The top and bottom walls consist of particles of diameter d_0 , in which the number of particles of each wall is N_w and their centers of gravity are located at $x_G^\pm(t) = \pm A \sin(\Omega t)$ and $y_G^\pm(t) = \pm L_y(t)/2$, with the amplitude A and angular frequency Ω of oscillation (see Fig.1). Since the system size $L_y(t)$ under the influence of the pressure P depends on time, we introduce an effective shear strain:

$$\gamma_{0,\text{eff}} := \frac{2A}{L_0}, \quad (1)$$

* daisuke.ishima@yukawa.kyoto-u.ac.jp

where L_0 is the linear size of the shear direction.

We adopt the equations of motion of the walls at $y_G^\pm(t)$:

$$m_w \frac{dv_{w,y}^\pm}{dt} = \pm(P_w^\pm - P)L_0 - \xi_d v_{w,y}^\pm, \quad (2)$$

where \pm , m_w , $v_{w,y}^\pm$, P_w^\pm , and ξ_d are indices referring to the wall at $y_G^\pm(t)$, mass of the wall $m_w = N_w m_0$, velocity in the y -direction of the wall at $y_G^\pm(t)$, internal pressure of the particles, and damping coefficient, respectively.

Let m_i , \mathbf{r}_i , $I_i = m_i d_i^2/8$, and ω_i be the mass, position, moment of inertia, and z -component of rotational velocity of particle i , respectively. The equations of motion for translation and rotation are, respectively, given by

$$m_i \frac{d^2 \mathbf{r}_i}{dt^2} = \sum_{j \neq i} \mathbf{f}_{ij}, \quad (3)$$

$$I_i \frac{d\omega_i}{dt} = \sum_{j \neq i} T_{ij}, \quad (4)$$

where we have introduced the contact force \mathbf{f}_{ij} and torque T_{ij} exerted by particle j on particle i . The torque T_{ij} in Eq. (4) satisfies

$$T_{ij} = -\frac{d_i}{2} \mathbf{f}_{ij} \cdot \mathbf{t}_{ij}, \quad (5)$$

where \mathbf{t}_{ij} is the tangential vector between particles i and j . We adopt the Cundall-Strack model for the contact force between particles [31, 32], where the contact force \mathbf{f}_{ij} is expressed as

$$\mathbf{f}_{ij} = (\mathbf{f}_{ij,n} + \mathbf{f}_{ij,t}) \Theta(d_{ij} - r_{ij}) \quad (6)$$

with $d_{ij} = (d_i + d_j)/2$ and $r_{ij} = |\mathbf{r}_i - \mathbf{r}_j|$. Here we have introduced the normal force $\mathbf{f}_{ij,n}$, the tangential force $\mathbf{f}_{ij,t}$, and Heaviside's step function $\Theta(x)$ satisfying $\Theta(x) = 1$ for $x \geq 0$ and $\Theta(x) = 0$ otherwise. The normal repulsive force is modeled as an elastic force with a linear spring constant k_n and the dissipative force with a damping constant ξ_n . Then, we model the normal force as

$$\mathbf{f}_{ij,n} = k_n \delta_{ij,n} \mathbf{n}_{ij} - \xi_n \mathbf{v}_{ij,n}, \quad (7)$$

where we have introduced $\mathbf{n}_{ij} = \mathbf{r}_{ij}/r_{ij}$ and $\mathbf{v}_{ij,n} = (\mathbf{v}_{ij} \cdot \mathbf{n}_{ij}) \mathbf{n}_{ij}$ with $\mathbf{r}_{ij} = \mathbf{r}_i - \mathbf{r}_j$, $\mathbf{v}_{ij} = d\mathbf{r}_{ij}/dt$ and $\delta_{ij,n} = d_{ij} - r_{ij}$. On the other hand, the tangential force $\mathbf{f}_{ij,t}$ takes two different expressions depending on the magnitude of the tangential force $\mathbf{f}_{ij,t} = |\mathbf{f}_{ij,t}|$:

$$\mathbf{f}_{ij,t} = \begin{cases} k_t \delta_{ij,t} \mathbf{t}_{ij} - \xi_t \mathbf{c}_{ij} & (f_{ij,t} < \mu f_{ij,n}), \\ \mu f_{ij,n} \mathbf{t}_{ij} & (\text{otherwise}), \end{cases} \quad (8)$$

where $\delta_{ij,t}$ is the tangential displacement between the particles. We have introduced the spring constant in the tangent direction k_t , damping coefficient in the tangent direction ξ_t , magnitude of the normal force $f_{ij,n} = |\mathbf{f}_{ij,n}|$, and tangential velocity at the contact point $\mathbf{c}_{ij} := \mathbf{v}_{ij} - \mathbf{v}_{ij,n} + \mathbf{t}_{ij}(d_i \omega_i + d_j \omega_j)/2$.

In our simulation, we adopt $k_t = k_n/2$, $\xi_n = (m_0 k_n)^{-1/2}$, $\xi_t = \xi_n$, and $\xi_d = \xi_n$ [13, 19]. The control parameters of our system are $\hat{P} := P/k_n$, $\gamma_{0,\text{eff}}$, $\Omega \sqrt{m_0/k_n}$, and μ . We deal with \hat{P} from 2.0×10^{-5} to 2.0×10^{-3} , $\gamma_{0,\text{eff}}$ from 1.0×10^{-6} to 1.0, and μ from 0 to 1.0. Furthermore, we mainly investigate that $N = 4,000$, and $\Omega/(2\pi) = 1.0 \times 10^{-4} \sqrt{k_n/m_0}$ in this paper. To know Ω dependences see Ref. [28].

To prepare the initial configuration, we place particles with diameters of $0.6d_0$, $0.5d_0$, $0.4d_0$, and $0.3d_0$ at random and then increase the diameter of the particles to reach the area fraction $\phi = 0.82$. Next, the pressure is applied to both walls to achieve a steady state. Then, oscillatory shear is applied through the walls [28]. We use the symplectic Euler method with the time step $\Delta t = 0.05 \sqrt{m_0/k_n}$.

We have averaged the data over 10 cycles after $N_{\text{ini}} = 10$ cycles to remove the effect of specific initial configurations. We set $t = 0$ at the moment of the end of N_{ini} cycles.

Let us introduce the area fraction $\phi(\Omega t, \hat{P}, \gamma_{0,\text{eff}})$

$$\phi(\Omega t, \hat{P}, \gamma_{0,\text{eff}}) = \frac{\sum_{i=1}^N \pi d_i^2 + N_w \pi d_0^2}{4L_x L_y(\Omega t, \hat{P}, \gamma_{0,\text{eff}})}. \quad (9)$$

To characterize the density change we also introduce $\delta\phi$:

$$\begin{aligned} \delta\phi(\hat{P}, \gamma_{0,\text{eff}}) &:= \phi(\Omega t = 2n\pi, \hat{P}, \gamma_{0,\text{eff}}) \\ &\quad - \phi(\Omega t = 2n\pi, \hat{P}, \gamma_{0,\text{eff}} = 0), \end{aligned} \quad (10)$$

where n is a non-negative integer. Since our system is confined by a constant pressure, the density depends on the time. Then, we focus on the excess fraction $\delta\phi$ at the instance of zero strain and the maximum strain rate.

III. RESULTS OF OUR SIMULATION

Let us present the results of our simulation for various μ . We found that dilatancy is always observable by increasing the strain amplitude (see Fig. 2). We also found that dilatancy is enhanced as the friction coefficient increases. This result may be related to the fact that the region of shear jamming is more extensive for large friction coefficients [13]. Note that the excess fraction $\delta\phi$ defined by Eq. (10) does not linearly decrease with the shear rate, as in the dilatancy observed in the steady sheared systems under constant pressures [19, 20]. It is noteworthy that compaction appears at an intermediate strain amplitude for small friction coefficients.

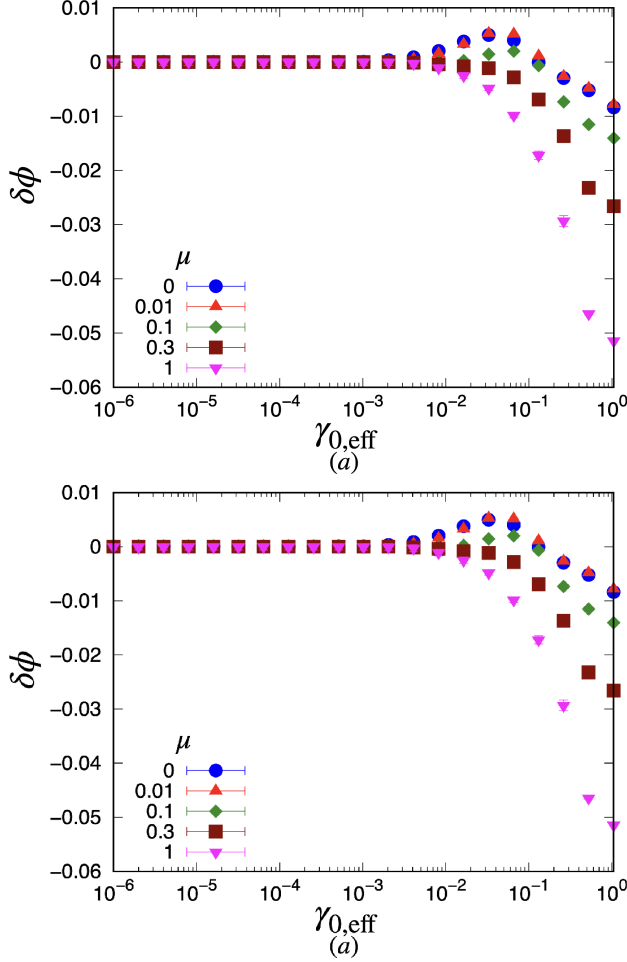


FIG. 2. Plots of $\delta\phi$ against $\gamma_{0,\text{eff}}$ for various μ at (a) $\hat{P} = 2.0 \times 10^{-3}$ and (b) $\hat{P} = 2.0 \times 10^{-4}$.

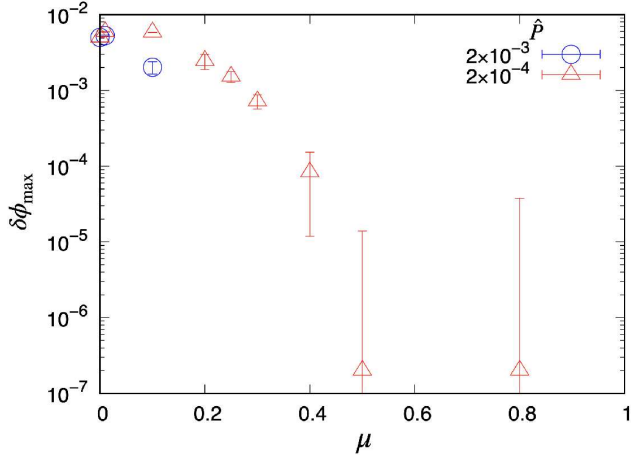


FIG. 3. Plots of $\delta\phi_{\text{max}}$ against μ for various \hat{P} .

To clarify the dependence of compaction on \hat{P} and μ , we plot $\delta\phi_{\text{max}}$, the maximum value of $\delta\phi$ at fixed \hat{P} , against μ for two different \hat{P} in Fig. 3. We confirm that $\delta\phi_{\text{max}}$ is almost independent of \hat{P} for $\mu \leq 0.01$ but it

strongly depends on the pressure for $\mu \geq 0.01$. Moreover, compaction disappears for $\mu > 0.1$ at $\hat{P} = 2 \times 10^{-3}$ while it survives even for $\mu = 0.8$ at $\hat{P} = 2 \times 10^{-4}$.

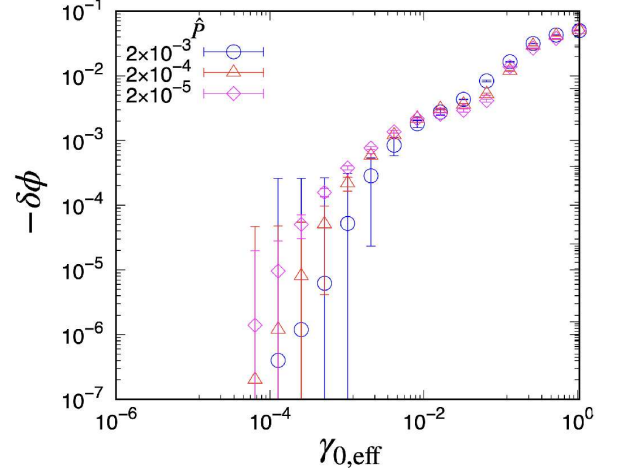


FIG. 4. Plots of $\delta\phi$ against $\gamma_{0,\text{eff}}$ for various \hat{P} at $\mu = 1.0$.

From now on, let us focus on the results for $\mu = 1.0$ to discuss the pressure dependence. From Fig. 4, $\delta\phi$ is zero for $\gamma_{0,\text{eff}} < 10^{-4}$, while it takes finite value. It is remarkable that $\delta\phi$ seems to depend on the pressure only little. In the previous paper [28], we reported that an appearance of a plastic flow can be understood by the behavior of the shear modulus. Similarly, the yielding strain γ^Y is proportional to the pressure, while the critical strain for dilatancy little depends on the pressure. Therefore, our result suggests that there is no direct connection between the density change and the behavior of shear modulus.

IV. CONCLUDING REMARKS

In conclusion, we conducted a numerical study of frictional granular systems under oscillatory shear confined by constant pressure. We found that compaction can be observed only for small μ at an intermediate strain amplitude, while dilatancy always takes place at large strain amplitude. We confirmed that dilatancy is a sort of continuous transition and little depends on the confined pressure.

One of the most important findings in this paper is that the density changes such as dilatancy and compaction are not directly connected with the yielding transition. Further investigation on the connection between two phenomena will be reported elsewhere.

Acknowledgement

The authors thank M. Otsuki and K. Saitoh for fruitful discussions and useful comments. This work is partially supported by the Grant-in-Aid of MEXT for Scientific Research (Grant No. 16H04025) and the Programs YITP-T-18-03 and YITP-W-18-17. The work of D.I. is partially supported by the Grant-in-Aid for Japan

Society for Promotion of Science JSPS Research Fellow (Grant No.20J20292). The research of H.H. has been partially supported by ISHIZUE 2020 of Kyoto University

Research Development Program.

-
- [1] E. Brown and H. M. Jaeger, Phys. Rev. Lett. **103**, 086001 (2009).
 - [2] M. Otsuki and H. Hayakawa, Phys. Rev. E **83**, 051301 (2011).
 - [3] R. Seto, R. Mari, J. F. Morris, and M. M. Denn, Phys. Rev. Lett. **111**, 218301 (2013).
 - [4] T. Kawasaki and L. Berthier, Phys. Rev. E **98**, 012609 (2018).
 - [5] D. Bi, J. Zhang, B. Chakraborty, and R. Behringer, Nature (London) **480**, 355 (2011).
 - [6] J. Zhang, T. Majmudar, and R. Behringer, Chaos **18**, 041107 (2008).
 - [7] J. Zhang, T. S. Majmudar, A. Tordesillas, and R. P. Behringer, Granul. Matt. **12**, 159 (2010).
 - [8] S. Sarkar, D. Bi, J. Zhang, R. P. Behringer, and B. Chakraborty, Phys. Rev. Lett. **111**, 068301 (2013).
 - [9] A. Fall, F. Bertrand, D. Hautemayou, C. Mezière, P. Moucheron, A. Lemaître, and G. Ovarlez, Phys. Rev. Lett. **114**, 098301 (2015).
 - [10] S. Sarkar, D. Bi, J. Zhang, J. Ren, R. P. Behringer, and B. Chakraborty, Phys. Rev. E **93**, 042901 (2016).
 - [11] I. R. Peters, S. Majumdar, and H. M. Jaeger, Nature (London) **532**, 214 (2016).
 - [12] D. Wang, J. Ren, J. A. Dijksman, H. Zheng, and R. P. Behringer, Phys. Rev. Lett. **120**, 208004 (2018).
 - [13] M. Otsuki and H. Hayakawa, Phys. Rev. E **101**, 032905 (2020).
 - [14] O. Reynolds, Philos. Mag. Ser. **20**, 469 (1885).
 - [15] R. A. Bagnold, Proc. R. Soc. London A **295**, 219 (1966).
 - [16] P. A. Thompson and G. S. Grest, Phys. Rev. Lett. **67**, 1751 (1991).
 - [17] H. M. Jaeger, S. R. Nagel, and R. P. Behringer, Rev. Mod. Phys. **68**, 1259 (1996).
 - [18] GDR MiDi, Eur. Phys. J. E **14**, 341 (2004).
 - [19] F. da Cruz, S. Emam, M. Prochnow, J. N. Roux and F. Chevoir, Phys. Rev. E. **72**, 021309 (2005).
 - [20] Y. Forterre and O. Pouliquen, Annu. Rev. Fluid Mech. **40**, 1 (2008).
 - [21] F. Boyer, É. Guazzelli and O. Pouliquen, Phys. Rev. Lett. **107**, 188301 (2011).
 - [22] J. B. Knight, C. G. Fandrich, C. N. Lau, H. M. Jaeger, S. Nagel, Phys. Rev. E **51**, 3957 (1995).
 - [23] E. R. Nowak, J. B. Knight, E. Ben-Naim, H. M. Jaeger and S. R. Nagel, Phys. Rev. E **57**, 1971 (1998).
 - [24] M. D. Haw, W. C. K. Poon, P. N. Pusey, Phys. Rev. E **57**, 6859 (1998).
 - [25] M. D. Haw, W. C. K. Poon, P. N. Pusey, P. Hebraud, F. Lequeux, Phys. Rev. E **58**, 4673 (1998).
 - [26] M. Nicolas, P. Duru, and O. Pouliquen, Eur. Phys. J. E **3**, 309 (2000).
 - [27] O. Pouliquen, M. Belzons, and M. Nicolas, Phys. Rev. Lett. **91**, 014301 (2003).
 - [28] D. Ishima and H. Hayakawa, Phys. Rev. E **101**, 042902 (2020).
 - [29] S. Luding, Phys. Rev. E **63**, 042201 (2001).
 - [30] M. Otsuki and H. Hayakawa, Phys. Rev. E **80**, 011308(2009).
 - [31] P. A. Cundall and O. D. L. Strack, Geotechnique **29**, 47 (1979).
 - [32] S. Luding, Granul. Matt. **10**, 235 (2008).